Electronic Supplementary Material (ESI) for Sustainable Energy & Fuels.

Electronic supplementary information

Derivative Voltammetry: a Simple Tool to Probe Reaction Selectivity in Photoelectrochemical Cell

Nukorn Plainpan, Florent Boudoire and Kevin Sivula*

Laboratory for Molecular Engineering of Optoelectronic Nanomaterials (LIMNO), École Polytechnique Fédérale de Lauanne (EPFL), Station 6, 1015 Lausanne, Switzerland.

Email: kevin.sivula@epfl.ch

Experimental details

Synthesis and fabrication of WO_3 electrode

The detail for the synthesis and the fabrication of the WO_3 electrode was reported in our previous publication.[1] In summary, the WO_3 precursor solution was synthesized via sol-gel method. The fabrication of the photoelectrode was performed via spin-coating of the WO_3 precursor solution onto a conductive FTO substrate followed by thermal annealing.

Characterization of WO_3 electrode

SEM micrograph

The top-down image illustrates the porous morphology of WO_3. The thickness of a WO_3 is found to be approximately 2 µm as measured in the cross-sectional image in **Figure S1B**. SEM micrography was performed using a Zeiss Merlin scanning electron microscope.

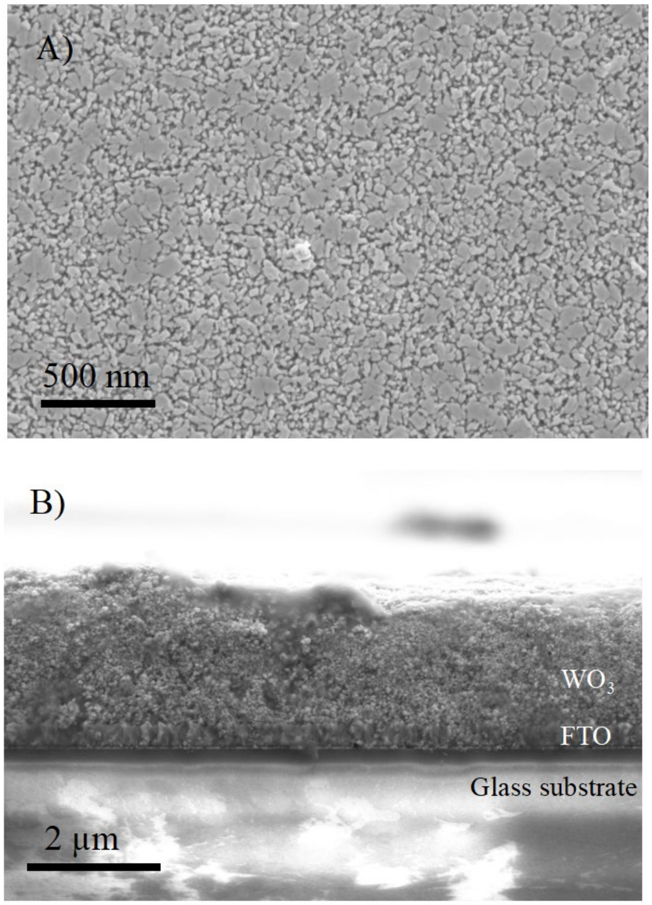

Figure S1 SEM images of WO_3 electrode. (A) top-down image and (B) cross-sectional image.

Raman spectroscopy

Raman spectrum was obtained using a LabRam spectrometer (Jobin Yvon Horiba). The excitation wavelength was at 532 nm. The observed spectrum corresponds well with the published spectrum in the literature.[2]

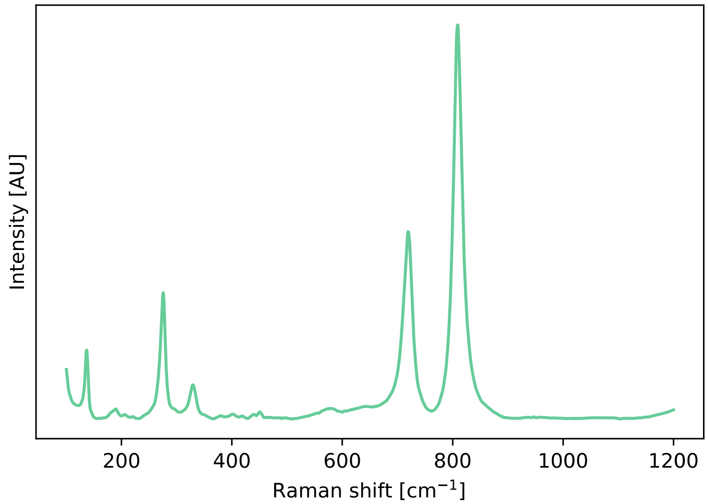

Figure S2 Raman spectrum of WO_3

XRD

XRD spectrum was obtained using a Panalytical Empyrean system (Theta-Theta, 240mm) equipped with a PIXcel-1D detector, Bragg-Brentano beam optics (including hybrid monochromator) and parallel beam optics. The spectrum correspond well with the reference spectrum found in the literature.[3]

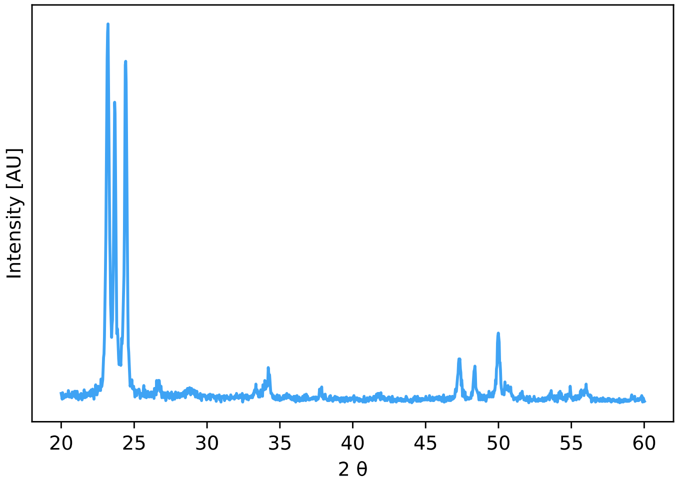

Figure S3 XRD pattern of WO_3

Standard electrochemical measurement

Unless otherwise noted, all electrochemical measurements were performed using a BioLogic SP-200 potentiostat in a three-electrode configuration. The working electrode, counter electrode and reference electrode were WO_3 on FTO, Pt wire and Ag/AgCl in saturated KCl solution respectively.

The condition NaP_i refers to a solution containing 0.1 M NaP_i, pH=4 solution and the condition HMF/NaP_i refers to a solution containing 5 mM HMF and 0.1 M NaP_i, pH=4. For all experiment involved illumination, a 1,000 W Xe lamp was used to simulate the solar spectrum. The illumination intensity was set at 1 sun and the direction of the illumination was from the back.

LSV experiment: Unless otherwise noted, all the LSV experiment were performed in a cappuccino cell. No agitation was given to the system during the LSV measurement, and the scan rate was set at 20 mV/s.

Photoelectrolysis experiment: All the photoelectrolysis experiment were performed in a custom-built glass cell. The electrode surface used was 2 cm^2. The electrolyte used was 5 mM HMF in 0.1 M NaP_i, pH=4 buffer (50 mL). The electrolyte solution was kept stirring throughout the experiment.

Product quantification

An aliquot of approximately 600 µL were periodically withdrawn from the reaction and was subjected to HPLC analysis (Shimadzu Prominence LC-20AP HPLC, equipped with dual UV-Vis detector set at 255 and 285 nm). Sulfuric acid (5 mM) was used as the mobile phase. The flow rate was kept at 0.5 $mL.min^{-1}$ (isocratic mode) and the column temperature was set at 40 ˚C. The aliquots were injected through polytetrafluoroethylene hydrophilic filter (0.22 µM pore size), to remove any highly retained compound, into a Coregel 87H3 7.8 × 300 mm column (part number CON-ICE-99-9861). The column was purchased from BGB Analytik AG, Switzerland. The calibration curve from the known compound was performed for the quantification and identification. The retention times for HMF was found to be 42.2 minutes.

Materials:

Unless otherwise noted, the following chemicals were used as received. HMF (99%) was purchased from Sigma-Aldrich. Sodium tungstate (99%) and Dowex® 50WX2, 100-200 mesh were obtained from Acros Organics.

Mathematical foundation of the fit ∂J/∂E

The mathematical expression used to create our fitting functions are modified from the literature.[4,5]

Consider Gericher's model for electron transfer in semiconductor

$$Rate\,of\,electron\,transfer\ = \int \kappa.f(E).DOS(E).D_{red}(E)dE \tag{1}$$

κ = electron transfer coefficient
$f(E)$ = Fermi-Dirac distribution function
$D_{red}(E)$ = Density of state of the reduced species in the solution.
E = Applied potential

In our condition, the following assumptions can be assumed:
i) $f(E)$ can be assumed to be constant as we constantly move the $E_{f,p}$ by sweeping the applied potential
ii) $D_{red}(E)$ can be assumed to be constant. $D_{red}(E)$ in our experiment is the concentration of HMF at the surface of the electrode. We demonstrate in **Figure S6** that our system is not mass transport limited. Hence, we can assumed that the concentration of HMF at the surface is in excess in comparison to the available holes at the surface. Hence, $D_{red}(E) \gg DOS(E)$, and $D_{red}(E)$ can be assumed to be constant.
iii) The rate of electron transfer = photocurrent (J)

Applying the three assumptions to **Equation 1** gives:

$$J = \kappa.f.D_{red}\int DOS(E)dE$$

Differentiate both sides of the equation with respective to E gives:

$$\frac{\partial J}{\partial E} = \kappa.f.D_{red} \times DOS(E)$$

As κ, f and D_{red} are all constant, we combine them into one constant, k_a.

$$\frac{\partial J}{\partial E} = k_a.DOS(E) \tag{2}$$

We assume $DOS(E)$ to have Gaussian distribution. Nevertheless, the simulated photocurrent obtained by integrating **Equation 2** do not represent the observed experimental photocurrent well in the saturated photocurrent region. The simulated photocurrent gives a constant value in the saturated photocurrent region. In the experimental photocurrent, the saturated photocurrent does not have a constant value but gradually increasing. We suspected that the built-in electric field from the band bending forces more holes to come to the surface, hence increasing the photocurrent. To improve our fitting, we add the second term to account for increasing hole flux due to the built-in electric field (drifting effect) from the band bending:

$$\frac{\partial J}{\partial E} = k_a.DOS(E) + k_b(E-E_{fb})^{-1/2}\int DOS(E)dE \tag{3}$$

k_b = Drifting constant
$(E-E_{fb})^{-1/2}$ = Magnitude of the space charge region. E_{fb} is the flat band potential. The value of E_{fb} = 0.45 V vs. RHE is used in all of our fitting
$\int DOS(E)dE$ = Number of the available states that the new arriving holes can participate in.

As mentioned earlier, we assume $DOS(E)$ to have Gaussian distribution. The expression can be written as:

$$DOS(E) = \frac{a}{\sigma\sqrt{(2\pi)}}exp(-\frac{(E-\mu)^2}{2\sigma^2}) \tag{4}$$

a = Magnitude of the peak
σ = Width of the peak
μ = Position of the peak

Our fitting function is obtained by substituting **Equation 4** into **Equation 3**. The constant k_a in **Equation 2** is combined with a in **Equation 4** to give the magnitude parameter, A. Our fitting function is described in **Equation 5**

$$\frac{\partial J}{\partial E} = \frac{A}{\sigma\sqrt{(2\pi)}}exp(-\frac{(E-\mu)^2}{2\sigma^2}) + k_b(E-E_{fb})^{-1/2}\int \frac{A}{\sigma\sqrt{(2\pi)}}exp(-\frac{(E-\mu)^2}{2\sigma^2})dE \tag{5}$$

Fitted Parameters

The parameters from the fit ∂J/∂E of NaP_i and HMF/NaP_i solution are as follows

	NaP_i	**HMF/NaP_i**
A1	n/a	0.323
$\sigma 1$	n/a	0.100
$\mu 1$	n/a	0.661
A2	1.080	1.040
$\sigma 2$	0.163	0.188
$\mu 2$	0.939	0.938
k_b	0.240	0.240

Table S1 Fitted parameters

Fitting ∂J/∂E of HMF/NaP$_i$ with only one fitting curve

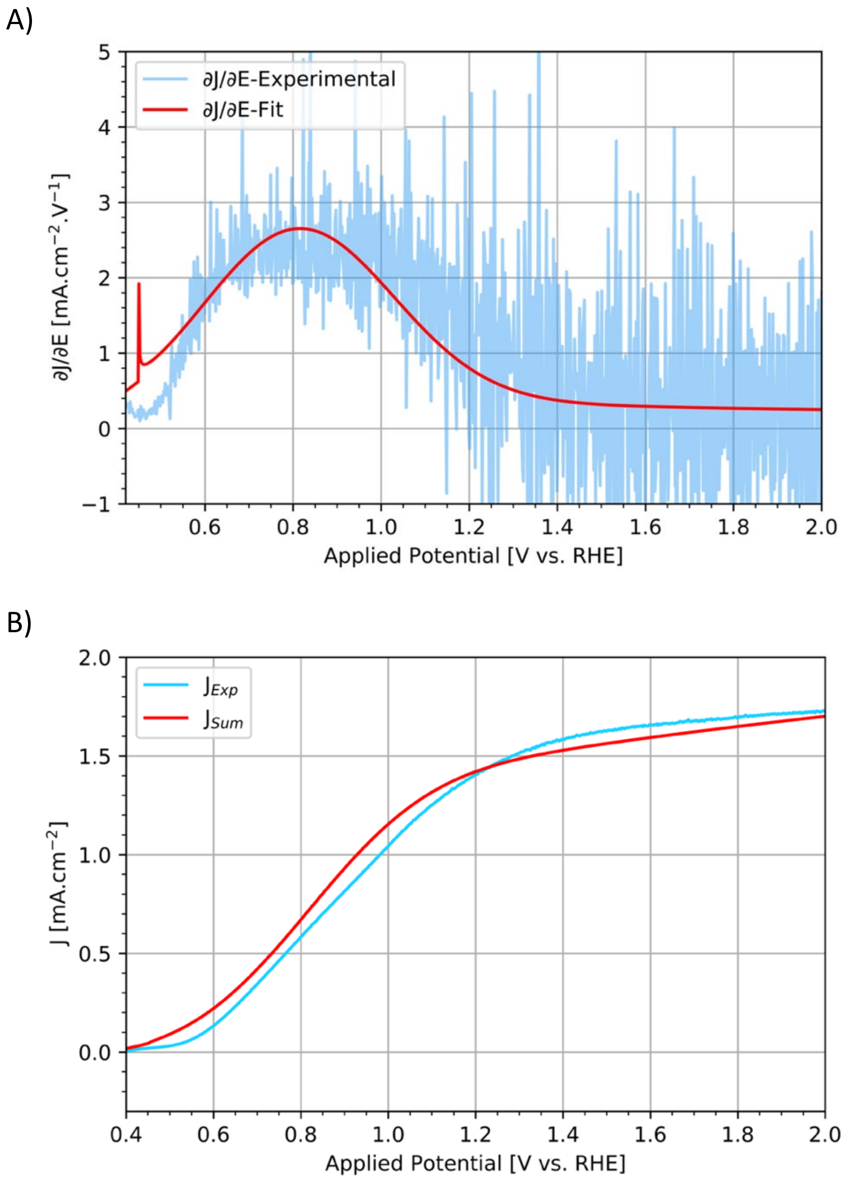

Figure S4 A) ∂J/∂E analysis and B) Simulated photocurrent of HMF/NaP$_i$ solution with only 1 fitting curve.

Schematic of HMF oxidation to FDCA

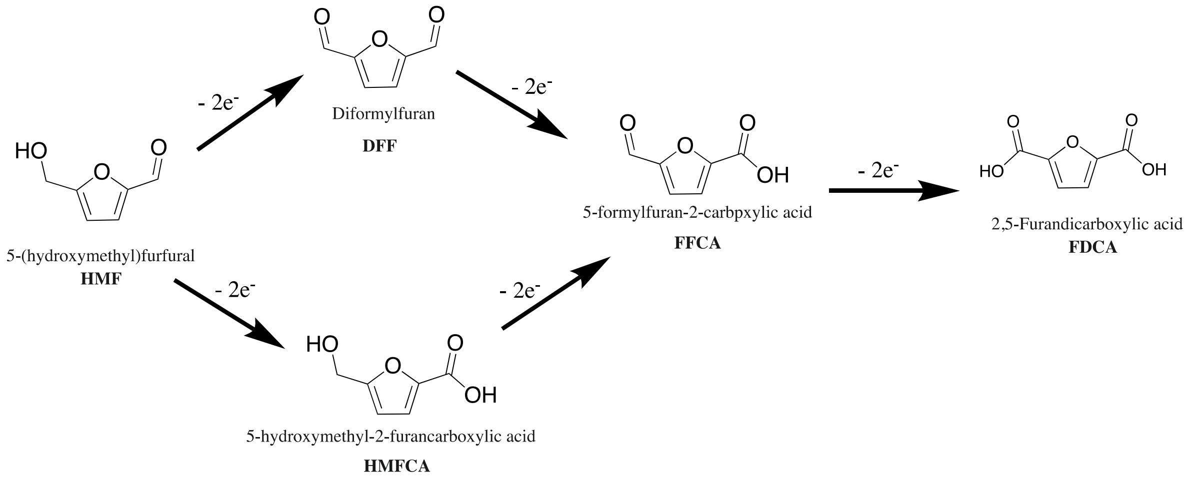

Figure S5 HMF oxidation reaction scheme

∂J/∂E of DFF/NaP$_i$ solution

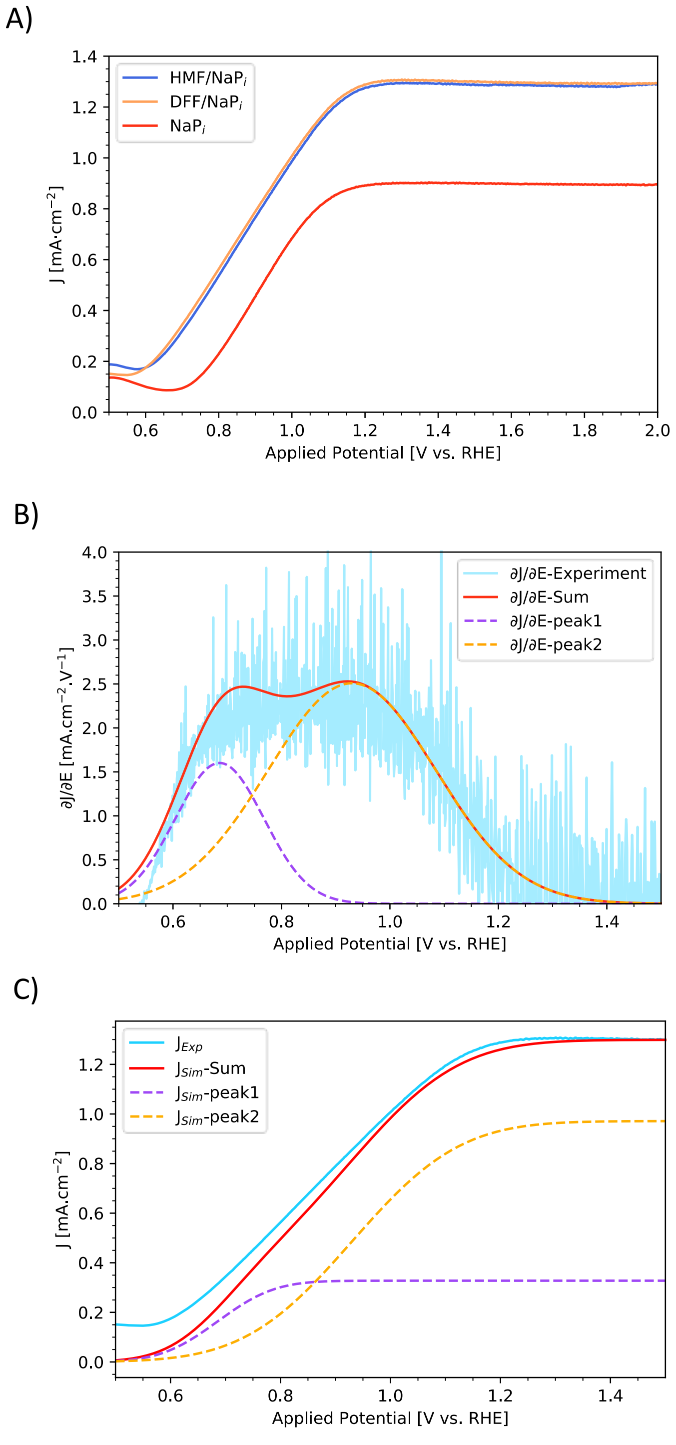

Figure S6 A) Linear sweep voltammogram of WO_3 in HMF/NaP$_i$, DFF/NaP$_i$ and blank (NaP$_i$) solution. B) The ∂J/∂E analysis for the DFF/NaPi case and C) the experimental and simulated photocurrent of WO_3 in DFF/NaP$_i$ solution (5 mM)

Effect of HMF concentration

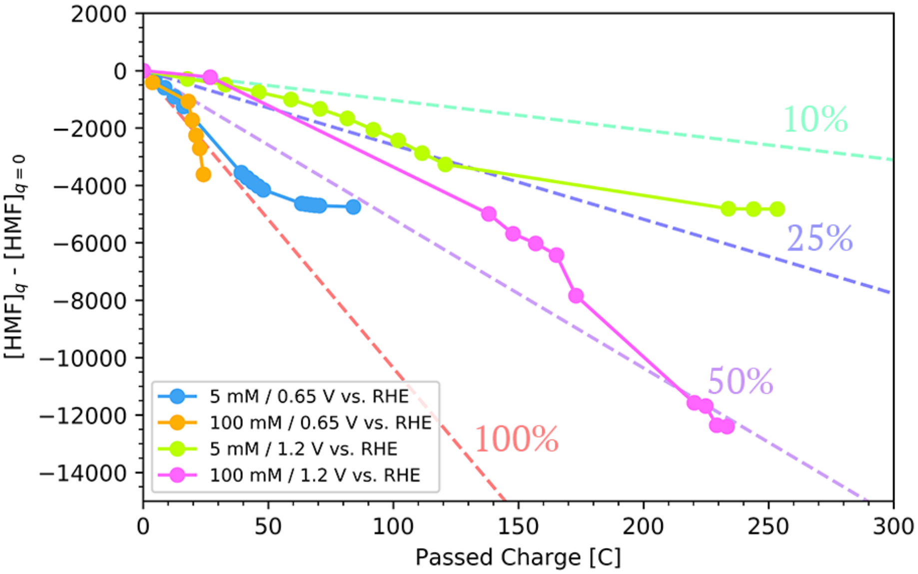

Figure S7 HMF consumption as the function of passed charge at 0.65 V and 1.20 V vs. RHE and at the initial HMF concentration of 5 mM and 100 mM. The dotted line represent the Faradaic efficiency of 10%, 25%, 50% and 100% as calculated from two-electron oxidation of HMF

EIS fitting

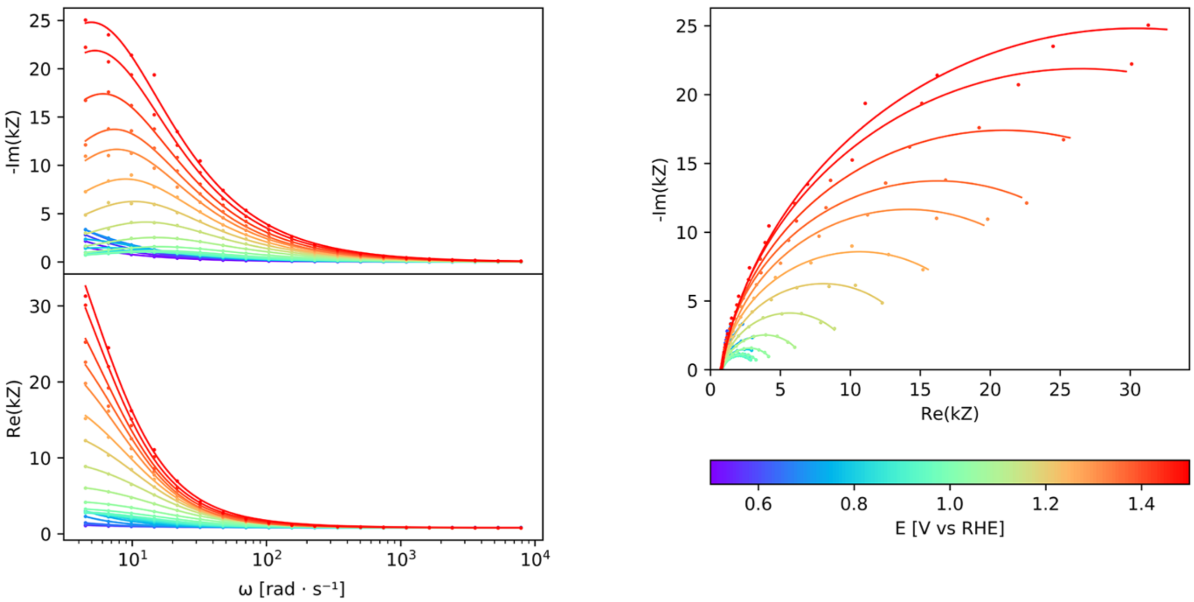

Figure S8 Bode plot (left) and Nyquist plot (right) in NaP_i electrolyte

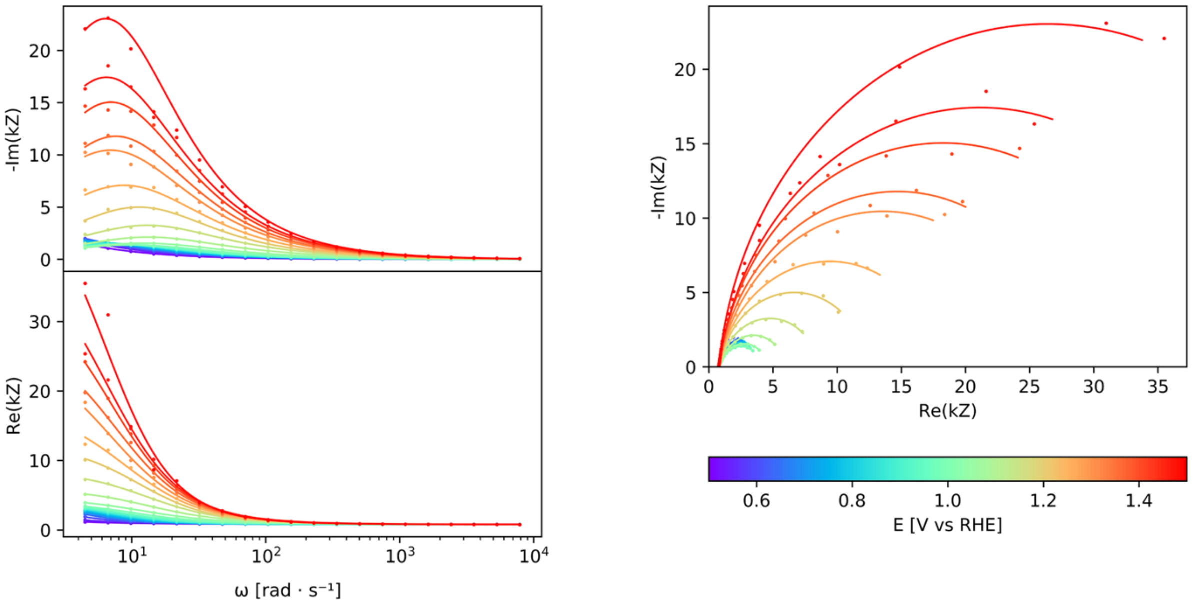

Figure S9 Bode plot (left) and Nyquist plot (right) in HMF/NaP_i solution

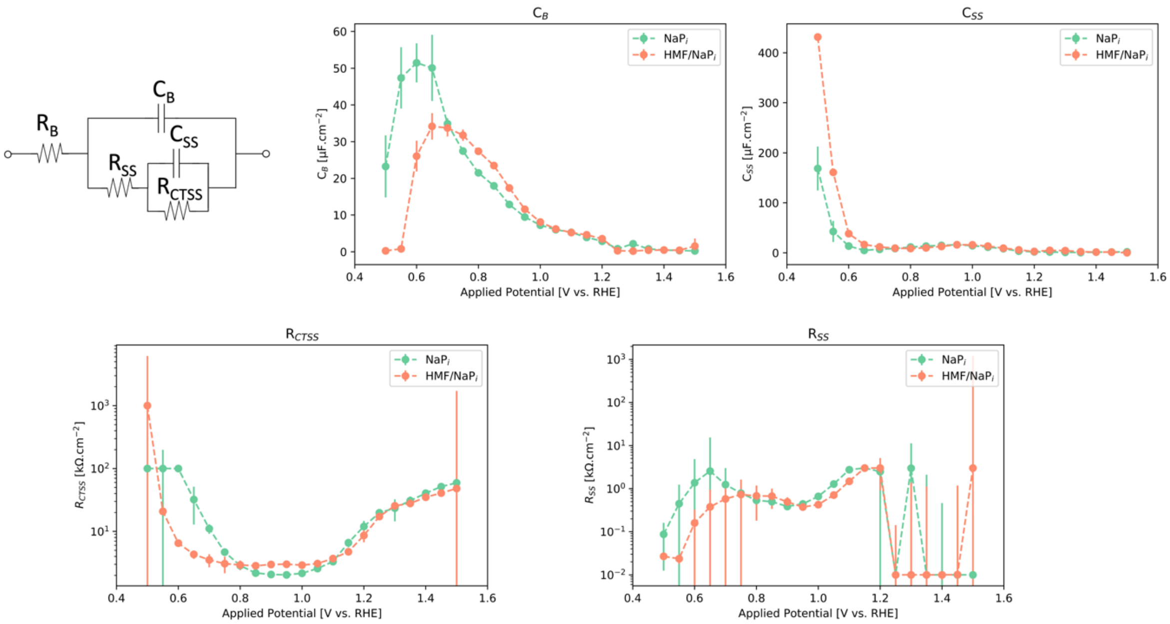

Figure S10 Equivalent circuit used in the fitting and the fitted value (C_b, C_{ss}, R_{CTSS} and R_{SS}) in NaP_i and HMF/NaP_i solution. The R_b value was kept constant at 0.79 kΩ.cm^{-2} for both solutions.

The fitted ∂J/∂E and the DOS(E) as probed from EIS

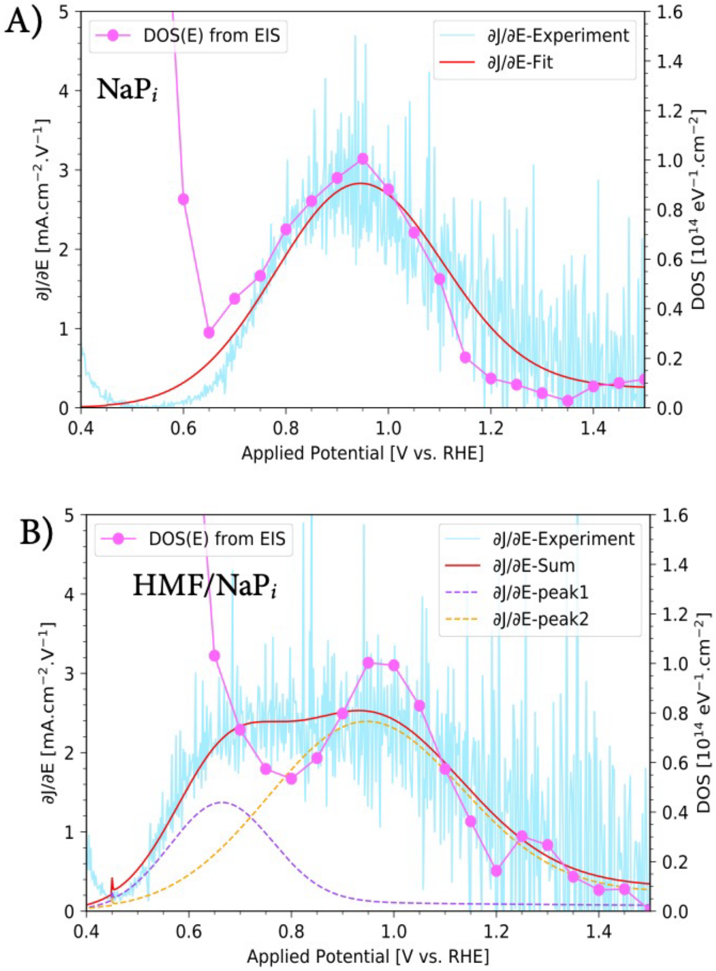

Figure S11 The overlaid graph of the experimental derivative voltammogram, the fit ∂J/∂E and the DOS(E) as found from EIS in A) NaP$_i$ electrolyte and B) 5 mM HMF in NaP$_i$ solution

References

1 C. R. Lhermitte, N. Plainpan, P. Canjura, F. Boudoire and K. Sivula, *RSC Adv.*, 2021, **11**, 198–202.

2 J. Díaz-Reyes, R. Castillo-Ojeda, M. Galván-Arellano and O. Zaca-Moran, *Advances in Condensed Matter Physics*, 2013, **2013**, 1–9.

3 F. Liu, X. Chen, Q. Xia, L. Tian and X. Chen, *RSC Adv.*, 2015, **5**, 77423–77428.

4 Z. Wang, F. Fan, S. Wang, C. Ding, Y. Zhao and C. Li, *RSC Adv.*, 2016, **6**, 85582–85586.

5 R. Memming, in *Semiconductor Electrochemistry*, Wiley-VCH Verlag GmbH & Co. KGaA, Weinheim, Germany, 2015, pp. 127–168.